Finite-temperature entanglement for low-dimensional quantum spin chains

Zhao-Yu Sun,[1] Kai-Lun Yao,[1,2,*] Wei Yao,[1] De-Hua Zhang,[1] and Zu-Li Liu[1]
[1]*Department of Physics, Huazhong University of Science and Technology, Wuhan 430074, China*
[2]*International Center for Materials Physics, Chinese Academy of Sciences, Shenyang 110016, China*
(Received 18 August 2007; revised manuscript received 5 November 2007; published 14 January 2008)

Based on transfer-matrix density matrix renormalization group (TMRG) method, a general procedure to calculate the finite-temperature pairwise entanglement of low-dimensional quantum chains is proposed. The reduced pairwise density matrix is reconstructed with TMRG, and measures of quantum entanglement can be calculated from the pairwise density matrix. The finite-temperature entanglement of the diamond chain model and the spin trimerized model, which are two typical models revealing 1/3 plateaus in the magnetization curves, is calculated. For the diamond chain model, the anisotropy coefficient Δ is found to have a great effect on the appearance of the magnetization plateau, and the plateau disappears when $\Delta=0.5$. Moreover, our results show that the pairwise entanglement can provide information complementary to that obtained from bulk properties. For the trimerized model, the temperature dependence of the pairwise entanglement is calculated, and the threshold temperature T_c, above which the thermal entanglement vanishes, is found to be independent of the external magnetic field B. In addition, the scaling behavior of the thermal entanglement is calculated in the Trotter space. With the augmentation of the system in the Trotter direction, we find that the low-temperature entanglement shows obvious variation in the vicinity of quantum phase transition (QPT) point B_c and converges fast in noncritical regions, which provides another way to identify QPT of one-dimensional quantum systems.

DOI: 10.1103/PhysRevB.77.014416 PACS number(s): 03.67.Mn, 75.10.Jm, 05.30.−d

I. INTRODUCTION

Quantum entanglement has attracted much interest in recent years. Its nonlocal connotation[1] is regarded as a valuable resource in quantum communication and information processing,[2,3] and provides new perspectives for various many-body systems. Many studies have been carried out to investigate the entanglement properties of low-dimensional quantum lattice systems.[4–20] For example, Osterloh *et al.*[19] reported that the pairwise entanglement of two nearest neighbors shows scaling behavior in the vicinity of quantum phase transition (QPT) point of the transverse-field Ising model. Legeza and Sólyom[16] proposed to use the two-site entropy to indicate QPT. Most of these works concentrated on the ground-state entanglement.

Thermal entanglement has also been discussed in some papers.[21–26] For example, Kamta and Starace[21] found that for a two-qubit anisotropic *XY* model, one is able to produce entanglement at any temperature T by adjusting the magnetic field strength. In most of these works, only very small systems were achievable. Recently, Li *et al.*[25] calculated the thermal-state entanglement of a quantum mixed spin chain with 128 spins in the vicinity of $T=0$ by quantum Monte Carlo method (QMC). For the isotropic mixed spin chains with SU(2) symmetry, the logarithmic negativity (a measure of entanglement; see Ref. 27 for more details.) between any two spins is related directly to the two-particle correlation function; therefore, QMC was adopted. With the temperature low enough, the reduced density matrix of any two spins can be expressed as the weighted sum of the reduced density matrices of the ground state and the first excited state. So, the thermal entanglement can be calculated through the lowest two energy levels of the system when T is very low.

In this paper, based upon transfer-matrix density matrix renormalization group (TMRG) method,[28–32] we propose another procedure to calculate the thermal entanglement of one-dimensional quantum chains. First, compared with density matrix renormalization group (DMRG) method, which could only deal with the ground-state entanglement at least in its simplest way, our method can be used to calculate the entanglement at finite temperature, and the thermodynamic limit can be exactly performed, thus avoiding extrapolation in size of the system. Second, compared with the above QMC method, which achieves very low temperature by combining the lowest two energy levels, the achievable temperature with our procedure will not be confined to very low temperature, as will be discussed in detail in Sec. II. Third, by reconstructing the pairwise density matrix, only the shift-invariance symmetry is needed to calculate the pairwise entanglement of one-dimensional (1D) quantum systems, and any other symmetry [such as SU(2)] is not necessary.

Low-dimensional quantum spin systems have been an intriguing subject in several decades. Among many achievements in this area, the phenomenon of the topological quantization of magnetization, especially the 1/3 magnetization plateau for the diamond chain[34] and the trimerized chain,[35] has been studied in many papers.[33–39] For example, the thermodynamic properties of spin-1/2 diamond chains have been studied in our previous work with Green's function method and TMRG method.[36,37] The reason why these lattice models have attracted so much attention is not only that the magnetization plateaus in these models reveal interesting quantum effect but also that they are not toy models. A magnetization plateau has been observed experimentally in $Cu_3(CO_3)_2(OH)_2$, which is regarded as a model substance of diamond chain,[40] and for the spin-1/2 trimer chain compound $Cu_3(P_2O_6OH)_2$, a plateau has also been observed.[41] We note that most theoretical studies about these models are concentrated on the magnetism and the thermodynamics,

while the quantum entanglement, which would surely provide another perspective on the quantum properties of the models, has not been discussed in detail. In this paper, we will study the thermal entanglement of these two models by TMRG. For the diamond chain model, the effect of the anisotropy coefficient Δ on the plateaus of the magnetization and the thermal entanglement is investigated, and it is found that the plateaus disappear when $\Delta=0.5$. In addition, the thermal entanglement is found to reveal some quantum information which cannot be obtained by studying the bulk properties of the chain. For the trimerized model, the thermal entanglement is calculated and the threshold temperature T_c, above which the thermal entanglement vanishes, is found to be independent of the magnetic field. Furthermore, with the increase of L, which denotes the size of the system in Trotter direction in TMRG procedure, it is found that the low-temperature entanglement is very sensitive to L in the vicinity of quantum critical fields and it converges fast in noncritical regions, which provides a new way to identify QPTs by analyzing low-temperature entanglements. An explanation will be given in the paper.

This paper is organized as follows. In Sec. II, we briefly outline the basic procedure to calculate the thermal entanglement with TMRG method. In Sec. III, the anisotropic diamond chain model is discussed. The thermal entanglement of the trimerized model is shown in Sec. IV, and a summary is given in Sec. V.

II. THERMAL ENTANGLEMENT WITH TRANSFER-MATRIX RENORMALIZATION GROUP METHOD

First, let us review how to calculate the pairwise entanglement between two $S=\frac{1}{2}$ spins at zero temperature. Though for some simple models the ground-state entanglement can be calculated through the differential of macroscopic thermodynamical functions,[11] a more general way of numerical calculation is to calculate the entanglement from the reduced density matrix.

In the standard basis $\{|\uparrow\uparrow\rangle, |\uparrow\downarrow\rangle, |\downarrow\uparrow\rangle, |\downarrow\downarrow\rangle\}$, the elements of pairwise reduced density matrix in the ground state can be expressed as correlation functions:[42,43]

$$\hat{\rho}_{i,j}=\begin{pmatrix} \langle P_i^{\uparrow}P_j^{\uparrow}\rangle & \langle P_j^{\uparrow}\sigma_j^{-}\rangle & \langle \sigma_i^{-}P_j^{\uparrow}\rangle & \langle \sigma_i^{-}\sigma_j^{-}\rangle \\ \langle P_i^{\uparrow}\sigma_j^{+}\rangle & \langle P_i^{\uparrow}P_j^{\downarrow}\rangle & \langle \sigma_i^{-}\sigma_j^{+}\rangle & \langle \sigma_i^{-}P_j^{\downarrow}\rangle \\ \langle \sigma_i^{+}P_j^{\uparrow}\rangle & \langle \sigma_i^{+}\sigma_j^{-}\rangle & \langle P_i^{\downarrow}P_j^{\uparrow}\rangle & \langle P_i^{\downarrow}\sigma_j^{-}\rangle \\ \langle \sigma_i^{+}\sigma_j^{+}\rangle & \langle \sigma_i^{+}P_j^{\downarrow}\rangle & \langle P_i^{\downarrow}\sigma_j^{+}\rangle & \langle P_i^{\downarrow}P_j^{\downarrow}\rangle \end{pmatrix}, \tag{1}$$

where $P^{\uparrow}=\frac{1}{2}(1+\sigma^z)$, $P^{\downarrow}=\frac{1}{2}(1-\sigma^z)$, and $\sigma^{\pm}=\frac{1}{2}(\sigma^x\pm i\sigma^y)$. The brackets denote the ground-state expectation values and σ are the Pauli matrices.

As the pairwise reduced density matrix can be calculated directly by tracing over all spins in the ground state except the two spins i and j, formula (1) is not used in most DMRG calculations. However, it is the starting point of our TMRG method to calculate the thermal entanglement of one-dimensional systems.

It is easy to prove that formula (1) still holds for finite temperature if the ground-state expectation is substituted by thermodynamic average value. All these expectation values at finite temperature can be calculated by means of TMRG method, then the pairwise density matrix can be reconstructed, and the measures of the entanglement can be calculated through the pairwise density matrix.

In TMRG calculations, a 1D infinite quantum system is transformed to a two-dimensional (2D) classical system with Trotter-Suzuki decomposition.[28–32] Low temperature is achieved by increasing the size (L) of the 2D classical structure in the Trotter direction, i.e., $T=\frac{1}{\epsilon L}$ (with ϵ a quantity defined in the Trotter-Suzuki decomposition). More details about TMRG method are discussed in Ref. 31.

For simplicity, let us consider the thermal average of a local operator $O_{i,i+1}$, which is defined at two nearest neighbors. Then, $\langle O_{i,i+1}\rangle$ can be calculated as

$$\begin{aligned}\langle O_{i,i+1}\rangle &= \lim_{N\to\infty}\frac{1}{Z}\mathrm{Tr}(T_M(O_{i,i+1})e^{-\beta H}) \\ &= \lim_{N\to\infty}\lim_{\epsilon\to 0}\frac{1}{Z}\mathrm{Tr}(T_M(O_{i,i+1})T_M^{N/2-1}) \\ &= \lim_{\epsilon\to 0}\frac{\langle\psi_{max}^{l}|T_M(O_{i,i+1})|\psi_{max}^{r}\rangle}{\lambda_{\max}},\end{aligned} \tag{2}$$

where T_M is the transfer matrix and $T_M(O_{i,i+1})$ is the modified transfer matrix with the operator $O_{i,i+1}$ included. λ_{max} is the leading eigenvalue of T_M, and $\langle\psi_{max}^{l}|$ and $|\psi_{max}^{r}\rangle$ are the corresponding left and right eigenstates. In this paper, we use N to denote the size of a quantum chain in real space and use L to denote the size of the 2D system in Trotter direction in TMRG procedure.

As the elements of the pairwise density matrix are correlation functions, it is easy to reconstruct the thermal pairwise density matrix from formula (2), and thus the measures of entanglement are achievable. The above discussion is confined to the entanglement of two $S=\frac{1}{2}$ spins, and similar procedure can be extended to mixed spin systems and high spin systems. Moreover, the pairwise entanglement of non-nearest neighbors is also achievable by calculating corresponding correlation functions. Thus, the method can be applied to general 1D quantum spin systems and can deal with many problems concerning finite-temperature entanglement.

In this paper, only the concurrence[4] of two nearest neighbors is considered. Let ρ_{ij} be the pairwise reduced density matrix obtained with TMRG, and let $\tilde{\rho}_{ij}$ be the spin-flipped matrix of ρ_{ij}, i.e., $\tilde{\rho}=\sigma_y\otimes\sigma_y\rho^{*}\sigma_y\otimes\sigma_y$, where σ_y is the Pauli matrix. Then, the concurrence is given through

$$\tilde{C}=\mu_1-\mu_2-\mu_3-\mu_4, \tag{3}$$

$$C=\max\{0,\tilde{C}\}, \tag{4}$$

where μ_i are the square roots of the four real eigenvalues of $\rho\tilde{\rho}$ in decreasing order. In this paper, we use $\tilde{C}$ in most cases and a negative $\tilde{C}$ denotes an unentangled state.

In our program, ϵ is fixed as 0.05, the maximum number of optimal states is taken as 100, and the maximum L achieved is 1000. In the calculations, the truncation error is

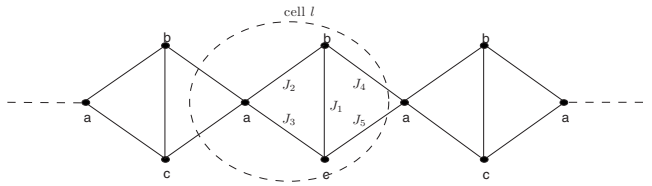

FIG. 1. Sketch of the diamond chain. Every cell contains three spins, labeled with a, b, and c.

found to be smaller than 10^{-9} in most cases, which shows that our results are well converged with the number of states kept.

III. ANISOTROPIC DIAMOND CHAINS

We consider a spin-1/2 diamond chain (see Fig. 1) with anisotropic Heisenberg interaction. The Hamiltonian of the chain with an external magnetic field B can be written as

$$H_{diamond} = \sum_{l=1}^{N} \left\{ \left[J_1 h_{lb,lc} + J_2 h_{la,lb} + J_3 h_{la,lc} + \frac{J_4}{2}(h_{(l-1)b,la} + h_{lb,(l+1)a}) + \frac{J_5}{2}(h_{(l-1)c,la} + h_{lc,(l+1)a}) \right] + B(S^z_{la} + S^z_{lb} + S^z_{lc}) \right\}, \quad (5)$$

where $h_{i,j} = S^x_i S^x_j + S^y_i S^y_j + \Delta S^z_i S^z_j$.

The system contains N cells ($N \to \infty$ in TMRG calculations) identified with l, and every cell contains three spins labeled with a, b, and c. Δ is the anisotropic coefficient ($\Delta \in [0,1]$). In our calculations, we adopt $J_1 = -3$ and $J_2 = J_3 = J_4 = J_5 = 1$. Phase diagram of diamond chains with isotropic Heisenberg interaction was in several papers,[34,36–38] and a 1/3 plateau in the magnetization curve was disclosed in some parameter region. A diamond chain with XY interaction was discussed in one of our recent papers [37] using the Green's function method, and a magnetization plateau was also observed. In this section, we discuss the effect of the anisotropic coefficient Δ on the magnetization plateau and the corresponding thermal-entanglement plateau. The model becomes an isotropic Heisenberg diamond model when $\Delta = 1$ and an XY diamond model when $\Delta = 0$.

In order to verify the validity of our thermal-entanglement procedure, we compare the low temperature results by TMRG with the zero-temperature results by DMRG in Fig. 2. Both the magnetization and the concurrence are plotted with $\Delta = 0$. In the DMRG calculations, the chain contains $N = 100$ cells with open boundary condition. Three QPT points are identified at $B_1 = 0.7$, $B_2 = 1.5$, and $B_3 = 2.2$. The magnetization shows a 1/3 plateau when $B_1 < B < B_2$ and saturates after $B > B_3$ (B_1 and B_2 denote the plateau region and B_3 denotes the saturation field), while the concurrence shows a relatively large value when $B_1 < B < B_2$ and it vanishes when $B > B_3$. In the TMRG calculations, we fix L as 300; thus, the temperature is $T = 0.067$. It shows that the low-temperature properties of the chain are in good agreement with the zero-temperature properties. The most apparent difference between the low-temperature results and the zero-temperature results happens in the vicinity of the three QPT points. At zero temperature, both the magnetization and the concurrence show singular points at the QPT points, while at low temperature, these singular points are smoothed by thermodynamic fluctuation. Figure 2 shows that our procedure to investigate the finite-temperature entanglement is feasible.

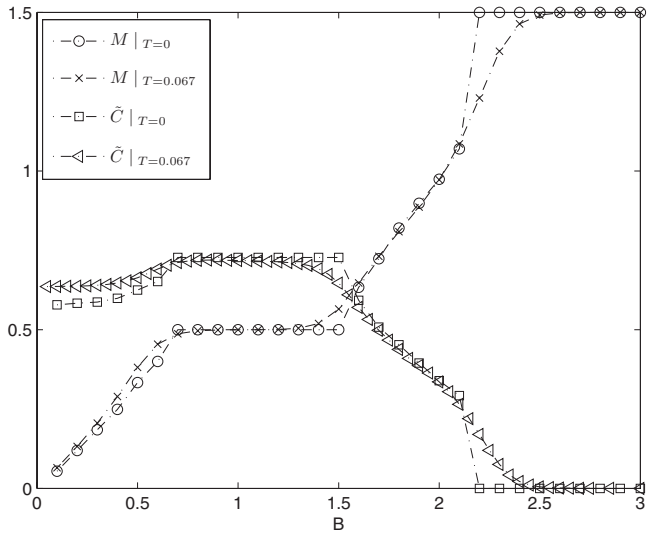

FIG. 2. M and $\tilde{C}$ vs B for the diamond chain with $\Delta = 0$. Both DMRG results ($T = 0$) and TMRG results ($T = 0.067$) are plotted, and three QPT points are identified ($B_1 = 0.7, B_2 = 1.5$, and $B_3 = 2.2$). It shows that the low-temperature results deviate from zero-temperature results obviously in the vicinity of the critical points. Relatively large difference between $\tilde{C}|_{T=0}$ and $\tilde{C}|_{T=0.067}$ is observed when B is small, which will be discussed in Sec. V.

The magnetization per cell of the anisotropic diamond chain is plotted in Fig. 3(a). The anisotropic efficient Δ changes from 0.0 to 1.0 with step of 0.1. The results are achieved with $L = 300$. When $\Delta = 0.0$, the system is an XY diamond chain, and the magnetization shows a 1/3 plateau when $B_1 < B < B_2$ ($B_1 = 0.7$ and $B_2 = 1.5$). Along with the increase of Δ, the gap between B_1 and B_2 decreases and the width of the 1/3 plateau is reduced gradually, and when $\Delta = 0.5$, the 1/3 plateau disappears. When $\Delta > 0.5$, the 1/3 plateau appears again, and its width is enhanced with the increase of Δ. When $\Delta = 1.0$, the system becomes an isotropic Heisenberg diamond chain, and the phase in which the magnetization increases from 0 to 0.5 disappears. In addition, the saturation filed B_3 is also influenced obviously by Δ. The concurrence between spin la and spin lb of the diamond chains is shown in Fig. 3(b). From up to bottom, Δ increases from 0.0 to 1.0 with step of 0.1. When $\Delta = 0.0$, $\tilde{C}$ shows a broad peak between B_1 and B_2. With the increase of Δ, the peak drops and the width of the peak decreases gradually. When Δ approaches 0.5, $\tilde{C}$ is monotonous in the vicinity of $B = 1.0$, and neither a broad peak nor a broad valley appears. When $\Delta > 0.5$, a broad valley appears between B_1 and B_2, and the width of the valley increases when Δ increases.

It is found that a study of entanglement can provide some information that cannot be obtained by studying macroscopic

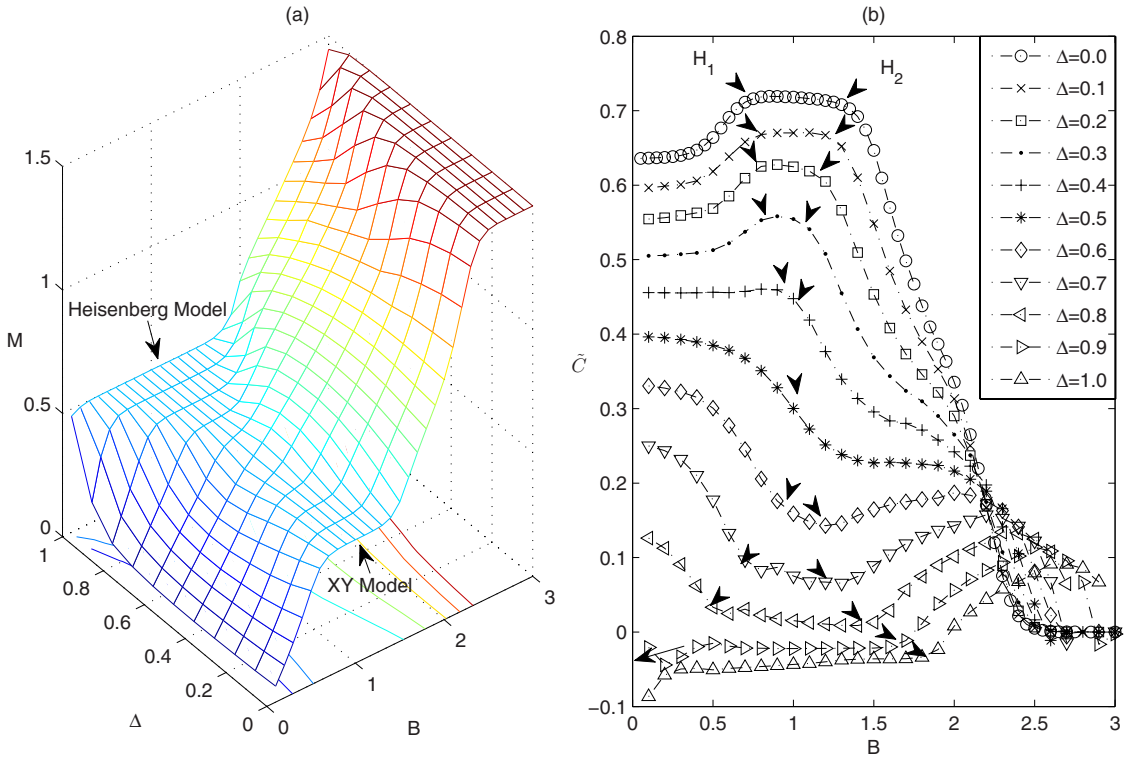

FIG. 3. (Color online) (a) Three-dimensional graph of the magnetization as a function of Δ and B for anisotropic diamond chains. It shows that Δ can influence the 1/3 magnetization plateau severely, and the plateau even disappears with $\Delta=0.5$. (b) $\tilde{C}$ as a function of B for different Δ.

thermodynamical quantities. We focus our attention on the 1/3-magnetization-plateau phase (with $B_1<B<B_2$). For the XY diamond chain (with $\Delta=0$), spins la and lb are unentangled with each other ($\tilde{C}$ is negative) in the 1/3-plateau state, and for the isotropic Heisenberg diamond chain ($\Delta=1$), they are highly entangled (the concurrence is about 0.7) in the 1/3-plateau state. It shows that these two plateau states cannot be distinguished from each other by the analysis of magnetization (as the magnetization is 0.5 in both states), but the analysis of entanglement can distinguish them. Thus, the study of quantum entanglement can provide some information complementary to that obtained from the magnetization. An explanation is given. Let ρ_l denote the reduced density matrix of the lth cell. For a fixed Δ, ρ_l does not show any change with B when $B_1<B<B_2$; thus, the magnetization and the concurrence, which can be calculated from ρ_l, keep constant (see Fig. 2). For a fixed B [for example, $B=1.0$ in Fig. 3(b)], ρ_l changes with Δ obviously; thus, the local quantities, such as the average magnetizations of spins a, b, and c ($\langle m_a\rangle$, $\langle m_b\rangle$, and $\langle m_c\rangle$, correspondingly), are functions of Δ in general. However, the magnetization per cell, i.e., $M=\langle m_a\rangle+\langle m_b\rangle+\langle m_c\rangle$, turns out to keep 1/2; thus, it cannot always detect the variation of $\langle m_i\rangle$ ($i=a$, b and c) and ρ_l. In order to see it more clearly, let us consider the simplest case and suppose the plateau state of the lth cell can be described appropriately with a pure-state wave function:[34,38]

$$|\varnothing_l\rangle = x|\uparrow\uparrow\downarrow\rangle + y|\uparrow\downarrow\uparrow\rangle + z|\downarrow\uparrow\uparrow\rangle, \tag{6}$$

with $x^2+y^2+z^2=1$. We find that the pairwise entanglement between spins a and b is $C_{ab}=|2yz|$ and that the magnetization of every spin can be expressed as $\langle m_a\rangle=1/2-z^2$, $\langle m_b\rangle=1/2-y^2$, and $\langle m_c\rangle=1/2-x^2$. It shows that C_{ab} and $\langle m_i\rangle$ ($i=a$, b and c) are sensitive to the variation of $|\varnothing_l\rangle$, while the magnetization per cell is equal to 1/2 for any x, y, and z. It is clear that as a consequence of summarizing and averaging, M can describe the average magnetization of the system very well, but it may not record all the information of local quantities of the chain. Thus, the concurrence, which is a local quantity describing the local quantum entanglement, can surely provide information complementary to that obtained from M.

IV. SPIN TRIMERIZED CHAINS

The spin trimerized chain is another model which can display 1/3 magnetization plateau and its thermodynamic properties have been discussed in several papers.[35,39] A simple trimerized spin-1/2 Heisenberg chain is defined by the Hamiltonian[39]

$$H_{trimerized} = \sum_{l=1}^{N} (JS_{lb}\cdot S_{lc} + JS_{lc}\cdot S_{la} + J'S_{la}\cdot S_{(l+1)b}) - B\sum_{l=1}^{N}(S_{la}^z + S_{lb}^z + S_{lc}^z). \tag{7}$$

The system is made up of N unit cells ($N\to\infty$ in TMRG calculations) identified with l, and every cell contains three

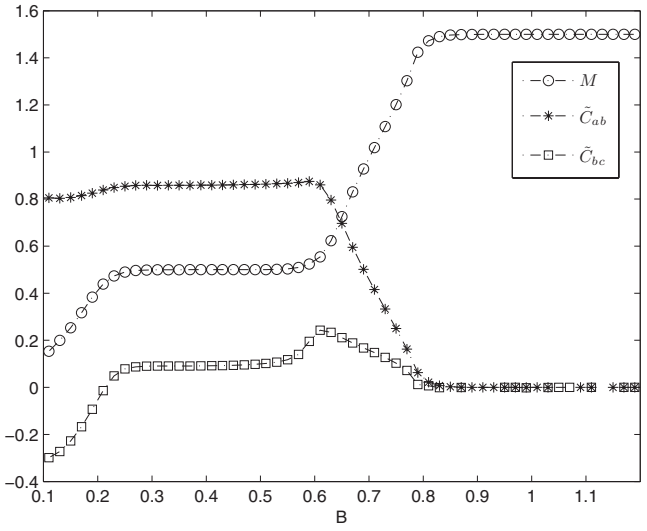

FIG. 4. M, $\tilde{C}_{ab}$, and $\tilde{C}_{bc}$ vs B with $T=0.02$ for the spin trimerized model.

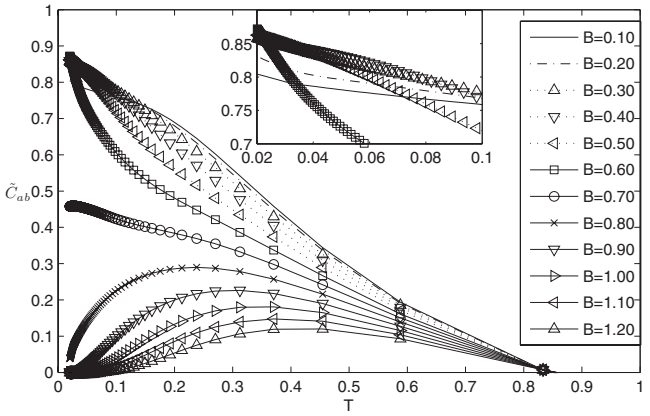

FIG. 5. $\tilde{C}_{ab}$ vs T for different B for the spin trimerized model. A critical temperature is observed at $T_c=0.85$ and the entanglement vanishes when $T>T_c$. The inset shows an enlargement of low-temperature and low-field region.

spins denoted as a, b, and c. The intracell exchange integral is J, and the intercell exchange integral is J', with $J(J')>0$ denoting the antiferromagnetic coupling and $J(J')<0$ denoting the ferromagnetic coupling. B is the external magnetic field. In our calculations, we choose $J=-1$ and $J'=1$; thus, the chain is an antiferromagnetic-antiferromagnetic-ferromagnetic trimerized chain. $L=1000$ is adopted in the calculations, and the lowest temperature achieved is 0.02.

In order to identify the phases of the system approximately, the magnetization and the pairwise entanglement with $T=0.02$ are plotted in Fig. 4. M is the magnetization per cell, $\tilde{C}_{ab}$ is the pairwise entanglement between la and $(l+1)b$, and $\tilde{C}_{bc}$ describes the pairwise entanglement between lb and lc. The magnetization shows a 1/3 plateau when $B_1<B<B_2$, with $B_1=0.26$ and $B_2=0.6$, and saturates after $B>B_3$, with $B_3=0.8$ (similar magnetization curve has been plotted in Ref. 39, which verifies our TMRG procedure once again). When $B<B_3$, the entanglement between la and $(l+1)b$ is found to be obviously larger than that between lb and lc. In addition, the turning points of $\tilde{C}_{ab}$ and $\tilde{C}_{bc}$ show good agreement with that of M. From formula (4), we can see that the turning points of C_{bc} would not be consistent with that of M, which suggests that at zero temperature, we cannot identify the QPT points of the system by analyzing the singular points of C_{bc} imprudently. This issue has been discussed in detail in Yang's paper.[11]

The temperature dependence of $\tilde{C}_{ab}$ is shown in Fig. 5. It shows clearly that there is a threshold temperature T_c ($T_c\simeq 0.85$). When $T>T_c$, the entanglement vanishes. We find that T_c is not affected by the magnetic field B. Furthermore, the monotonicity of $\tilde{C}_{ab}$ depends on B. When $B\geqslant 0.8$ (B_3), with T decreasing from T_c to 0.02, the entanglement first increases to a finite value and then decreases to zero. When $B\leqslant 0.7$, with the decrease of T, $\tilde{C}_{ab}$ increases monotonously. The other two critical points cannot be identified by analyzing the monotonicity of the entanglement.

Now, let $|\tilde{C}'|$ be the magnitude of $\frac{\partial \tilde{C}_{ab}}{\partial T}$. $|\tilde{C}'|_{B=B_2}$ and $|\tilde{C}'|_{B=B_3}$ is very large at low temperature. For $B=B_1$, from the inset of Fig. 5, it can be seen that $|\tilde{C}'|_{B=B_1}$ ($B_1=0.2$) is larger than $|\tilde{C}'|_{B=0.1}$ and $|\tilde{C}'|_{B=0.3}$ for low temperature. These results suggest that at very low temperature, $\frac{\partial \tilde{C}}{\partial T}$ shows extreme value in the vicinity of the critical field, which can be used to identify QPT of the chain.

It has been studied in several papers that in real space, the scaling behavior of the ground-state entanglement entropy can be used to identify a QPT:[6] In the vicinity of a QPT, the entanglement entropy increases gradually with the increase of N, and in a noncritical region, it converges vary fast. Now, we will propose a similar behavior in the Trotter space. As has been explained, in TMRG calculations, the 2D checkerboard structure is enhanced gradually in the Trotter direction (in other words, L increases). In Fig. 6, the magnetization M and the entanglement $\tilde{C}_{ab}$ are plotted as functions of L for different B. Figure 6(a) shows clearly that for noncritical magnetic fields, M converges very fast with the increase of L, while for critical fields $B=B_1$, B_2, and B_3 ($B_1=0.2$, $B_2=0.6$, and $B_3=0.8$ approximately), the magnetization does not converge when L achieves 1000. $\tilde{C}_{ab}$ shows similar behavior for critical fields B_2 and B_3. In the vicinity of B_1, though the behavior is not very obvious, $|\tilde{C}'|_{B=0.2}$ is larger than $|\tilde{C}'|_{B=0.1}$ and $|\tilde{C}'|_{B=0.3}$ (also see the inset of Fig. 5).

Now we will give an explanation why $\tilde{C}_{ab}$ tends to vary evidently with L in the vicinity of critical points while converges fast in noncritical fields. In other words, what we need to understand is the response of $\tilde{C}_{ab}$ to change of the temperature for different B. At low temperature (L is very large), the reduced density matrix of any two spins can be expressed as the weighted sum of the reduced density matrices of the lowest energy states. For simplicity, we only consider the ground state and the first excited state; thus, the reduced density matrix can be expressed as[25]

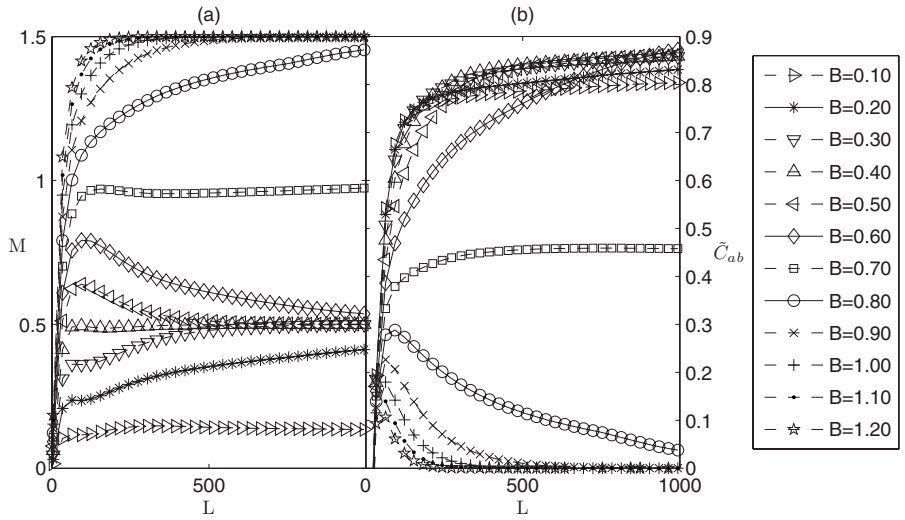

FIG. 6. (a) M and (b) $\tilde{C}_{ab}$ vs L for different B for spin trimerized models. B is scanned from 0.1 to 1.2 with step of 0.1. It shows that in noncritical region, M and $\tilde{C}_{ab}$ converge fast, while in the vicinity of QPT points (B=0.2, 0.6, and 0.8 approximately), they do not converge with L=1000.

$$\rho_{i,i+1} = \frac{1}{Z}e^{-\beta H} \approx \frac{1}{Z}(\omega_g \rho_g + \omega_1 \rho_1), \tag{8}$$

where ρ_g and ρ_1 are the pairwise density matrices of the ground state and the first excited state, and the corresponding weights are $\omega_g = e^{-\beta E_g}$ and $\omega_1 = e^{-\beta E_1}$.

Let us define $D = E_1 - E_g$ (Ref. 44); thus, formula (8) can be expressed as

$$\rho_{i,i+1} = \frac{1}{Ze^{\beta E_g}}(\rho_g + e^{-\beta D}\rho_1). \tag{9}$$

Any point of nonanalyticity in the ground state energy of the infinite lattice system should be identified as a QPT point: The nonanalyticity could be either the limiting case of an avoided level crossing, or an actual level crossing;[45] thus, D decreases gradually as B approaches B_c (in both cases) and even vanishes (in the level-cross case).

Our discussion is confined in low-temperature region, so β is very large. With noncritical B, D is finite and $e^{-\beta D}$ is very small; thus, ρ_1 will contribute little to $\rho_{i,i+1}$ and the ground state is the only effective ingredient in $\rho_{i,i+1}$. In other words, $\rho_{i,i+1}$ suffers little influence of thermodynamic fluctuation. While in the vicinity of a critical field, D achieves a minimum value and $e^{-\beta D}$ achieves a maximum value ($e^{-\beta D} \sim 1$ in the level-cross case), then the excited state can give effective contribution to $\rho_{i,i+1}$, and $\rho_{i,i+1}$ is more sensitive to the temperature. It shows that $\rho_{i,i+1}$ tends to be influenced by β more sensitively in the critical field than in the noncritical region, and that is why thermal entanglement can be used to identify a QPT.

It has to be mentioned that two different channels are adopted by DMRG and TMRG to identify the QPT point of the system. Generally, QPT point is identified by studying the analyticity of the ground-state entanglement in the thermodynamic limit. In DMRG calculations, as it deals with the ground state of the system, what one needs to do is to enlarge the chain (by increasing N) to approach the thermodynamic limit, while in TMRG calculations, as an infinite chain is considered directly, one needs to lower the temperature of the system (by increasing L) to approach zero temperature. Moreover, DMRG uses the singularity of the ground-state energy to identify a QPT, while TMRG uses the decrease of the energy gap between the ground state and excited states to identify a QPT.

With the increase of N (in DMRG) and L (in TMRG), the scaling behaviors of the zero-temperature entanglement and the thermal entanglement are established. It can be seen that there are some similarities between these two scaling behaviors. Both the zero-temperature entanglement and the thermal entanglement converge fast in noncritical regions and do not converge in critical regions. It has to be mentioned that these similar behaviors are caused by different reasons. The divergence of zero-temperature entanglement in critical regions is related to the fact that the zero-temperature correlation function shows singular behavior in the vicinity of a QPT point, while the nonconvergence of the thermal entanglement in critical regions, as has been explained, results from the reduction of the energy gap (D) between the ground state and the excited states when B approaches B_c. Furthermore, there is obvious difference between the two scaling behaviors. In most cases, the zero-temperature block entropy would increase logarithmically with the augmentation of N, while Fig. 6(b) shows that the thermal entanglement decreases with the increase of L when $B > 0.80$. It is known that the ground-state entanglement of many 1D quantum systems shows similar scaling behaviors, and we think the intrinsic reason for this similarity is that these scaling behaviors are established in similar physical processes, i.e., the growth of the systems. As the scaling behavior of the thermal entanglement is established in a different physical process (explicitly, it is established along with the cooling of the system), we think it should be comprehensible for the thermal entanglement to behave differently from the zero-temperature entanglement, and we cannot establish a direct relation between the two scaling behaviors, especially in simple mathematical form.

V. DISCUSSION AND SUMMARY

It should be noted that although TMRG is very powerful in calculating the magnetization, the result for the thermal

entanglement is not very precise when the external magnetic field B is small. The magnetization depends on the diagonal elements of the pairwise density matrix and the thermal entanglement depends on all the elements of $\hat{\rho}_{i,j}$. We find that with a small B, the error in calculating the nondiagonal elements is much larger than that in calculating diagonal elements. We can see from Fig. 6 that B_2 and B_3 are easy to be identified while B_1 is not conspicuous. In addition, in Fig. 2, when B is small ($B<0.5$), the difference between the concurrence calculated by DMRG and that by TMRG is evident. Nevertheless, the results for larger B are credible.

In summary, we have proposed a method to calculate the finite-temperature entanglement for 1D quantum spin systems. Compared with normal DMRG method, which only deals with the zero-temperature entanglement for finite 1D systems, our procedure deals with infinite 1D quantum chains directly and the entanglement properties at finite temperature are achievable. In addition, compared with the QMC method, which can only achieve very low temperature by calculating the first excited state,[25] our method can calculate the thermal entanglement at any finite temperature. With this method, the effect of the anisotropic parameter Δ on the magnetization and the entanglement of the diamond chain is investigated. The anisotropy is found to influence the 1/3 magnetization plateau and the entanglement plateau significantly. In addition, in the 1/3-magnetization-plateau phase, the entanglement varies with Δ, which suggests that the entanglement can reveal some quantum information that cannot be obtained by studying macroscopic thermodynamical quantities. In the spin trimerized model, the critical temperature T_c is found to be independent of B, and more work needs to be done to understand this result. Furthermore, corresponding to the scaling behavior of the ground-state entanglement entropy, a similar behavior for finite-temperature entanglement is established in Trotter space, which provides another way to identify QPTs of 1D quantum systems.

ACKNOWLEDGMENTS

It is a pleasure to thank Xing Xia for fruitful discussions. This work was supported by the National Natural Science Foundation of China (No. 10574047 and No. 10574048) and from Major Project of the National Natural Science Foundation of China (No. 20490210). This work is also supported by the National 973 Project under Grant. No. 2006CB921605.

*Corresponding author. klyao@mail.hust.edu.cn

[1] A. Einstein, B. Podolsky, and N. Rosen, Phys. Rev. **47**, 777 (1935).
[2] C. H. Bennett and D. P. DiVincenzo, Nature (London) **404**, 247 (2000).
[3] C. H. Bennett, D. P. DiVincenzo, J. A. Smolin, and W. K. Wootters, Phys. Rev. A **54**, 3824 (1996).
[4] W. K. Wootters, Phys. Rev. Lett. **80**, 2245 (1998).
[5] P. Lou and J. Y. Lee, Phys. Rev. B **74**, 134402 (2006).
[6] G. Vidal, J. I. Latorre, E. Rico, and A. Kitaev, Phys. Rev. Lett. **90**, 227902 (2003).
[7] S. J. Gu, S. S. Deng, Y. Q. Li, and H. Q. Lin, Phys. Rev. Lett. **93**, 086402 (2004).
[8] P. Zanardi, Phys. Rev. A **65**, 042101 (2002).
[9] J. Zhao, I. Peschel, and X. Q. Wang, Phys. Rev. B **73**, 024417 (2006).
[10] N. Laflorencie, E. S. Sørensen, M. S. Chang, and I. Affleck, Phys. Rev. Lett. **96**, 100603 (2006).
[11] M. F. Yang, Phys. Rev. A **71**, 030302(R) (2005).
[12] S. J. Gu, H. Q. Lin, and Y. Q. Li, Phys. Rev. A **68**, 042330 (2003).
[13] J. Vidal, G. Palacios, and R. Mosseri, Phys. Rev. A **69**, 022107 (2004).
[14] J. K. Stockton, J. M. Geremia, A. C. Doherty, and H. Mabuchi, Phys. Rev. A **67**, 022112 (2003).
[15] X. G. Wang and B. C. Sanders, Phys. Rev. A **68**, 012101 (2003).
[16] Ö. Legeza and J. Sólyom, Phys. Rev. Lett. **96**, 116401 (2006).
[17] L. A. Wu, M. S. Sarandy, and D. A. Lidar, Phys. Rev. Lett. **93**, 250404 (2004).
[18] N. Lambert, C. Emary, and T. Brandes, Phys. Rev. Lett. **92**, 073602 (2004).
[19] A. Osterloh, L. Amico, G. Falci, and R. Fazio, Nature (London) **416**, 608 (2002).
[20] E. Fradkin and J. E. Moore, Phys. Rev. Lett. **97**, 050404 (2006).
[21] G. L. Kamta and A. F. Starace, Phys. Rev. Lett. **88**, 107901 (2002).
[22] D. Gunlycke, V. M. Kendon, V. Vedral, and S. Bose, Phys. Rev. A **64**, 042302 (2001).
[23] X. G. Wang, Phys. Rev. A **66**, 044305 (2002).
[24] L. Zhou, H. S. Song, Y. Q. Guo, and C. Li, Phys. Rev. A **68**, 024301 (2003).
[25] S. B. Li, Z. X. Xu, J. H. Dai, and J. B. Xu, Phys. Rev. B **73**, 184411 (2006).
[26] J. Cao, X. L. Cui, Z. Qi, W. G. Lu, Q. Niu, and Y. P. Wang, Phys. Rev. B **75**, 172401 (2007).
[27] G. Vidal and R. F. Werner, Phys. Rev. A **65**, 032314 (2002); K. Audenaert, J. Eisert, M. B. Plenio, and R. F. Werner, *ibid.* **66**, 042327 (2002).
[28] S. R. White, Phys. Rev. Lett. **69**, 2863 (1992); Phys. Rev. B **48**, 10345 (1993).
[29] U. Schollwöck, Rev. Mod. Phys. **77**, 259 (2005).
[30] R. J. Bursill, T. Xiang, and G. A. Gehring, J. Phys.: Condens. Matter **8**, L583 (1996).
[31] X. Wang and T. Xiang, Phys. Rev. B **56**, 5061 (1997).
[32] N. Shibata, J. Phys. Soc. Jpn. **66**, 2221 (1997).
[33] M. Oshikawa, M. Yamanaka, and I. Affleck, Phys. Rev. Lett. **78**, 1984 (1997).
[34] K. Okamoto, T. Tonegawa, Y. Takahashi, and M. Kaburagi, J. Phys.: Condens. Matter **11**, 10485 (1999); K. Okamoto, T. Tonegawa, and M. Kaburagi, *ibid.* **15**, 5979 (2003).
[35] B. Gu, G. Su and S. Gao, J. Phys.: Condens. Matter **17**, 6081 (2005).
[36] K. L. Yao, Q. M. Liu, and Z. L. Liu, Phys. Rev. B **70**, 224430 (2004).

[37] H. H. Fu, K. L. Yao, and Z. L. Liu, Phys. Rev. B **73**, 104454 (2006).
[38] B. Gu and G. Su, Phys. Rev. B **75**, 174437 (2007).
[39] B. Gu, G. Su, and S. Gao, Phys. Rev. B **73**, 134427 (2006).
[40] H. Kikuchi, Y. Fujii, M. Chiba, S. Mitsudo, T. Idehara, T. Tonegawa, K. Okamoto, T. Sakai, T. Kuwai, and H. Ohta, Phys. Rev. Lett. **94**, 227201 (2005).
[41] M. Hase, M. Kohno, H. Kitazawa, N. Tsujii, O. Suzuki, K. Ozawa, G. Kido, M. Imai, and X. Hu, Phys. Rev. B **73**, 104419 (2006).
[42] X. G. Wang, Phys. Rev. A **66**, 034302 (2002).
[43] O. F. Syljuåsen, Phys. Rev. A **68**, 060301(R) (2003).
[44] Here, we use the weighted sum of the lowest two energy states to describe the low-temperature pairwise density matrix and it is believed that the physical essence has already been grasped. Strictly speaking, formula (8) is more suitable for a finite system, and for an infinite system the formula should be written in the form of the integral of the low energy bands, because the energy eigenvalue spectrum of an infinite system is continuous in most cases. Then, the state density ϱ as a function of the external field B, instead of $D(B)$, should be adopted in order to explain the temperature response of the entanglement. It has to be mentioned that at very low temperature, $D(B) \sim \frac{1}{\varrho(B)}$ and the two have similar physical essence; thus, we adopt formula (8) to explain the problem and it is very concise.
[45] Subir Sachdev, *Quantum Phase Transitions* (Cambridge University Press, Cambridge, 1999), Chap. 1.